The C-Terminal Half of the Anti-Sigma Factor FlgM Contains a Dynamic Equilibrium Solution Structure Favoring Helical Conformations†

Gary W. Daughdrill,‡ Linda J. Hanely, and Frederick W. Dahlquist*

Institute of Molecular Biology, University of Oregon, Eugene, Oregon 97403

Received August 7, 1997; Revised Manuscript Received November 12, 1997

ABSTRACT: FlgM is the inhibitor of σ^{28}, a transcription factor specific for the expression of bacterial flagella and chemotaxis genes. FlgM is also exported from the cytoplasm to the outside of the cell during the process of flagella filament assembly. In the absence of its targets, FlgM is a dynamic, mostly unfolded, molecule [Daughdrill, G. W., et al. (1997) *Nat. Struct. Biol. 4(4)*, 285−291]. The NMR resonance assignments, dynamics, and average secondary structure of this mostly unfolded form of FlgM are reported here. Because of the dynamic behavior of FlgM, the deviation of C_α chemical shifts from the random coil values was used to test for the presence of secondary structure [Wishart, D. S., and Sykes, B. D. (1994) *Methods Enzymol. 239*, 363−392]. This analysis shows two contiguous regions in the C-terminal half of FlgM with helical C_α chemical shifts. These two regions, M60−G73 and A83−A90, contained less than 10 medium-range NOEs, and the ^{15}N relaxation parameters suggest the helical structure is not rigid. However, the C_α chemical shifts of M60−G73, A83−A90, and other residues in the C-terminal half of FlgM shift toward their canonical random coil values with the addition of a chemical denaturant. Along with the values of the order parameter, S^2, this observation suggests the C-terminal half of FlgM exists in an equilibrium structural state that is nonrandom. The same analysis of the N-terminal half of FlgM suggests it more closely resembles a random coil in conditions with and without denaturant. It appears the C-terminal half of FlgM lacks sufficient intramolecular contacts to form stable secondary or tertiary structures. It is known this C-terminal region becomes rigidly held when FlgM binds σ^{28} (Daughdrill et al., 1997), and it is possible that binding stabilizes the helical structure. The potential evolutionary relationship between the inhibitory interaction of FlgM with σ^{28} and the autoinhibition observed in σ^{70} is discussed.

FlgM is a negative regulator of flagella and chemotaxis genes in *Escherichia coli* and *Salmonella typhimurium* (*1*). It performs this function by binding and inhibiting σ^{28}, the sigma factor responsible for the transcription of flagella and chemotaxis genes (*2*). When FlgM is not bound to σ^{28}, it is exported outside of the cell by the flagella export apparatus (*3*, *4*). A detailed NMR analysis performed on FlgM demonstrated it is mostly unfolded in the absence of σ^{28}. In the presence of σ^{28}, the C-terminal half of FlgM becomes structured, and the N-terminal half remains unfolded (*5*). Based on these data, we proposed that the structural states of free and bound FlgM are important for its flagella-specific export and like to think the biological function of FlgM depends on it being mostly unfolded (*5*). This proposal is consistent with the general assumption that the unfolded state is necessary for the translocation of most proteins (*6*).

The details of the structural rearrangement that occurs, when the C-terminal half of FlgM binds to σ^{28}, are unclear. However, one factor that differentiates the binding of a protein like FlgM, from a folded protein, is the apparent change in conformational entropy experienced by most of the amino acid residues involved in binding (*7*−*9*). One can imagine this process will play a critical role in determining the strength of the interaction because the loss of conformational entropy that occurs when residues are immobilized will reduce the binding affinity (*10*). This mechanism may serve to modulate biological activity by creating perturbations in the binding affinity that are on the order of the energy it takes to immobilize a single amino acid residue. Furthermore, Schulz (*11*) suggested that when folding and binding are coupled, natural selection can operate separately on affinity and specificity and that this separation is necessary for the evolution of complex biological systems. An extension of this hypothesis is: The specificity of an interaction can be increased without an increase in binding affinity if there is a compensating loss in conformational entropy. This may allow FlgM to more easily discriminate between the various sigma factors in the cell without sacrificing the ability to dissociate at a physiologically reasonable rate.

It is becoming more clear that mostly unfolded proteins like FlgM cannot be modeled as statistical random coils (*12*, *13*). Through the use of multidimensional NMR, methods that permit a reasonable structural description of the "conformational sets" in which a mostly unfolded protein exists are now available. These methods allow the identification of average secondary structure through the use of chemical shift information and the extraction of molecular tumbling

† This work was supported by NIH Grant AI 17808 to F.W.D.

* Author to whom correspondence should be addressed. Phone: (541) 346-5882. Facsimile: (541) 346-5891. E-mail: fwd@nmr.uoregon.edu.

‡ Current address: Department of Biology, University of Utah, Salt Lake City, UT 84112.

S0006-2960(97)01952-1 CCC: $15.00
Published on Web 01/13/1998

behavior from relaxation parameters (*14*−*16*). When applied to FlgM, these methods gave structural information about the flexible regions that fold in the presence of σ^{28} and permitted an estimation of the conformational entropy loss for the binding process.

MATERIALS AND METHODS

FlgM Sample Preparation. All FlgM samples were prepared as described in Daughdrill et al. (*5*). All experiments on FlgM were acquired on a single 10 mM uniformly ^{15}N-labeled sample or a 5 mM uniformly ^{13}C/^{15}N-labeled sample in 10 mM sodium phosphate, pH 6.2, 10 mM sodium chloride, 0.02% sodium azide, 10.0% D_2O, 25 °C, or 10 mM sodium acetate, pH 5.0, 10 mM sodium chloride, 0.02% sodium azide, 10.0% D_2O, 25 °C. FlgM samples were exchanged into urea-containing buffers using a 5 mL spin/desalting column packed with fine G-25 Sephadex (Sigma).

NMR Spectroscopy. The 3D ^{1}H−^{15}N NOESY-HSMQC[1] experiments are a variation of the 3D NOESY-HMQC sequences written by Marion et al. (*17*) and Zuiderweg and Fesik (*18*). The mixing time for the NOE effect was 200 ms, and the experiment was acquired as a complex matrix of 1024 × 512 × 128 points. The 3D ^{1}H−^{15}N TOCSY-HSMQC sequences were performed as described in Cavanagh et al. (*19*) and Marion et al. (*20*) and acquired as a complex matrix of 1024 × 512 × 128 points. The TOCSY and NOESY spectra were acquired with 16 scans per increment and spectral widths of 1612.9 Hz in F_1 and 6666.6 Hz in F_2 and F_3. The carrier frequencies were centered at 119 ppm in F_1 and 4.78 ppm in F_2 and F_3. The sensitivity-enhanced HNCO and HNCACB sequences were performed as described in Muhandiram and Kay (*21*) and Kay et al. (*22*). They were acquired as 64 × 32 × 512 and 128 × 48 × 512 complex points, respectively, using 8 scans per increment. The carrier frequencies for the HNCO and HNCACB were centered at 43.0 (F_1), 119.0 ppm (F_2), and 4.78 ppm (F_3). The spectral widths for the HNCO were 2000 (F_1), 1500 (F_2), and 8000 Hz (F_3). The spectral widths for the HNCACB were 9000 (F_1), 2000 (F_2), and 8000 Hz (F_3). The gradient ^{1}H−^{15}N HSQC sequences were performed as described in Bodenhausen and Ruben (*23*) and Kay et al. (*24*). The spectrum was acquired as a matrix of 512 × 1024 complex points using 16 scans per increment. The spectral widths used were 1612.9 Hz in F_1 and 6666.6 Hz in F_2. The carrier frequencies were centered at 119 ppm in F_1 and 4.78 ppm in F_2. The spin-lattice relaxation times (T_1), spin−spin relaxation times (T_2), and ^{1}H−^{15}N NOEs were measured by inverse-detected two-dimensional NMR methods using sequences developed by Kay et al. (*15*). Spin−lattice relaxation times were determined by collecting 7 two-dimensional spectra using relaxation delays of 14, 126, 238, 364, 547, 855, and 1206 ms. Spin−spin relaxation times were determined by collecting 8 two-dimensional spectra using spin-echo delays of 7.6, 30.5, 68.8, 100, 152, 198.6, 343.8, and 496.6 ms. Peak volumes from each series of relaxation experiments were fit to a single decaying exponential, and all errors derived from the fit were within 5% of reported values (data not shown). To measure the ^{1}H−^{15}N NOEs, one spectrum was acquired with the NOE effect, and another without the NOE effect for reference. For all experiments, water suppression was achieved using pulsed field gradients or presaturation. All the data except the HNCO and HNCACB experiments were acquired on a General Electric Omega 500 MHz spectrometer. The HNCO and HNCACB experiments were acquired on a Varian Inova 600 MHz spectrometer. All data were processed using the FELIX software from Hare Research and BioSym Technologies, San Diego, CA.

Relaxation Data Analysis. Relaxation data were analyzed using the "model free" approach of Lipari and Szabo (*14*). Equations and parameters relating T_1, T_2, and the NOE factor of an amide ^{15}N spin to the values of the spectral density function were identical to eqs 1−3 of Kay et al. (*15*). In the interpretation of the relaxation data, it is assumed the relaxation properties of the ^{15}N spins are governed solely by the ^{1}H−^{15}N dipolar coupling and the chemical shift anisotropy (CSA) interaction. Anisotropy in the tumbling was ignored [(*15*); this assumption is likely to be invalid for a mostly unfolded protein like FlgM, but the analysis ultimately provides a useful qualitative picture of its tumbling behavior]. Using these assumptions, a spherical molecule with an overall correlation time, τ_m, and an effective correlation time for rapid internal motions, τ_e, will have a spectral density function of the following form (*14*):

$$J(\omega) = S^2\,\tau_m/[1 + (\omega\tau_m)^2] + (1 - S^2)\tau/[1 + (\omega\tau)^2] \quad (1)$$

where $1/\tau = 1/\tau_m + 1/\tau_e$, and S^2 is the generalized order parameter, which describes the amplitude of internal motions. To a first-order approximation, the contribution of the fast internal motions to the spectral density can be ignored and permits the calculation of τ_m and S^2 from the T_1/T_2 ratio (*15*). Spectral density mapping was performed using a FORTRAN program written by Hongjun Zhou. The program first extracts the spectral density values for $J(0)$ and $J(\omega_N)$ from T_1 and T_2 values, ignoring the terms $J(\omega_H)$, $J(\omega_H-\omega_N)$, and $J(\omega_H+\omega_N)$. Then, the program assumes $J(\omega_H) = J(\omega_H-\omega_N) = J(\omega_H+\omega_N)$ and extracts $J(0)$, $J(\omega_H)$, and $J(\omega_N)$ from the T_1, T_2 and ^{1}H−^{15}N NOE values. The calculated errors due to the approximations mentioned above are generally less than 0.5%.

RESULTS AND ANALYSIS

FlgM Resonance Assignments. The assigned ^{15}N−^{1}H correlation spectrum of FlgM is shown in Figure 1. Backbone resonance assignments were made using a series of three-dimensional experiments that are described under Materials and Methods. From these data, ^1H_N, ^{15}N, $^{13}C_\alpha$, and $^{13}C_\beta$ resonance assignments were obtained for 88 of the 93 non-proline residues in FlgM and are listed in the supporting information (see Supporting Information Available). Two residues at the N-terminus as well as K32, M51, and Q52 were not assigned.

Average Secondary Structure of FlgM. For rigid helical regions in a protein, medium range NOEs are observed between the α hydrogen of a given residue and the amide [$d_{\alpha N}(i,i+3)$]or β [$d_{\alpha\beta}(i,i+3)$] hydrogens of the residue three positions away in the sequence (*25*). An analysis of the 3D ^{1}H−^{15}N NOESY spectrum for FlgM revealed less than 10 unambiguous medium-range NOEs, all of which were located

[1] Abbreviations: CSI, chemical shift indexes; NOESY, nuclear Overhauser enhancement spectroscopy; TOCSY, total correlation spectroscopy.

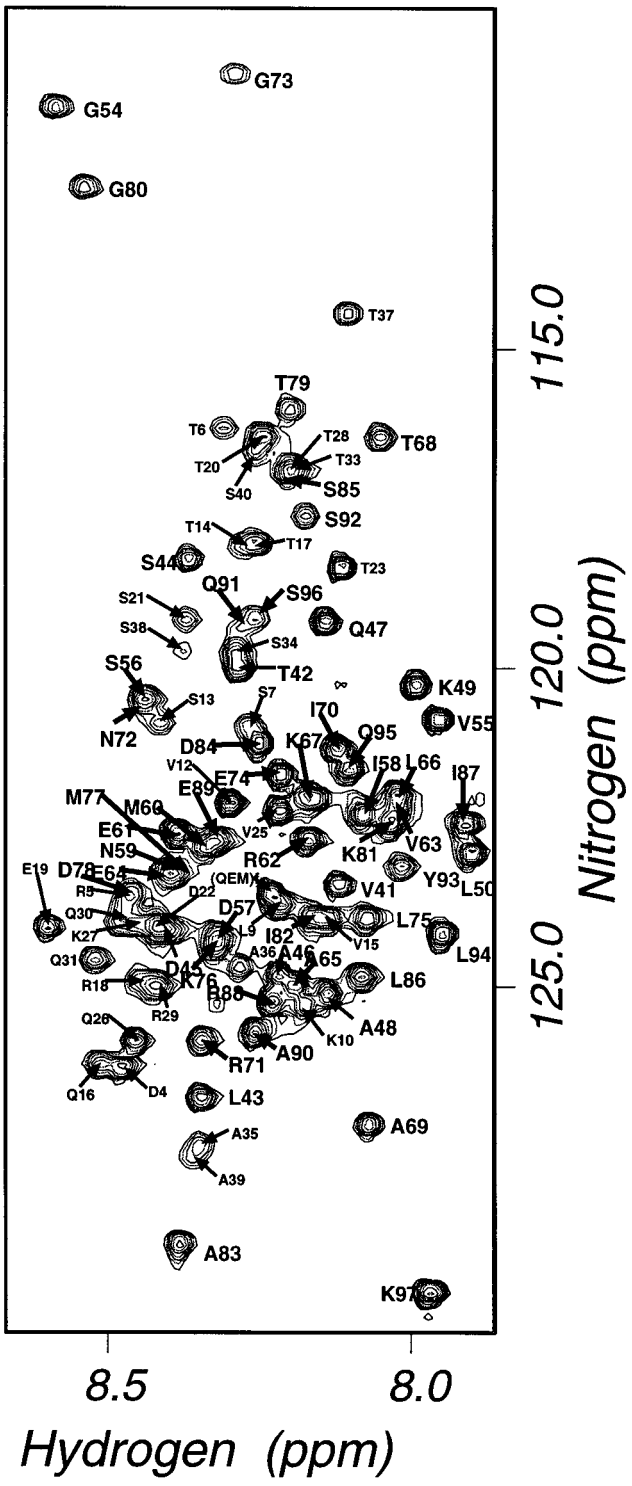

FIGURE 1: $^{15}N-^{1}H$ correlation spectrum of 2 mM ^{15}N-labeled FlgM in 10 mM sodium acetate at pH 5.0, 25 °C. Assignments of the backbone amide peaks corresponding to the residues in the partially folded region of the protein (V41−K97) are indicated in large type. Assigned residues from the unfolded N-terminal half of FlgM as well as unassigned residues that are also in this region are indicated by the smaller font.

in the C-terminal half of the molecule. Three were between I82/S85, D84/I87, and I87/A90, and four were between A65/T68 and I70/G73 (data not shown). This information suggests that there is some helical structure present in the C-terminal half of FlgM.

To further test for the presence of helical structure in the C-terminal half of FlgM, the deviation of C_α chemical shifts from the random coil values was calculated for the 88 assigned residues. The identification of secondary structure is possible based on these deviations (*16*). The results are shown in Figure 2 with the parts per million (ppm) difference from random coil plotted on the vertical axis, and the residue number plotted on the horizontal axis. The clear bars represent FlgM C_α chemical shifts in the absence of denaturant, and the black bars are chemical shifts in the presence of 7.5 M urea. The horizontal line at 0.80 ppm represents the cutoff for the helical chemical shift index (CSI). Because the C-terminal half of FlgM is only partially folded, any helical structure is likely the result of chemical shift averaging from multiple conformations. Therefore, it is inappropriate to characterize the helical structure present in FlgM in terms of the CSI. However, inclusion of the cutoff point in Figure 2 is useful to show the 'relative helicity' of FlgM residues. There appear to be two sequential regions from about M60−G73 and A83−A90 with helical chemical shifts that deviate significantly from the random coil value. A significant deviation has a chemical shift difference greater than the CSI cutoff and extends over at least one helical turn (3−4 residues).

Equilibrium Unfolding of FlgM. To test whether the chemical shift deviations for C-terminal FlgM residues represent an ensemble of nonrandom conformational states, the C_α chemical shifts were measured in the presence of increasing concentrations of the denaturant urea. The observed transitions for several residues are illustrated in Figure 3. The horizontal axis is the molar concentration of urea, and the vertical axis is the normalized C_α chemical shifts. The C_α chemical shifts were normalized by taking the difference between a residue's C_α chemical shift at all urea concentrations and the C_α chemical shift at 7.5 M urea. For each residue, this value was then divided by the difference in C_α chemical shift at 0 and 7.5 M urea. This process corrected for perceived differences in the shapes of the curves in Figure 3 that resulted from real differences in the range of chemical shifts observed for each residue.

In Figure 3, the data for two residues from the helical regions, I87 and S85, and two residues outside the helical regions, L50 and T79, are shown. All other residues in the C-terminal half of FlgM, for which assignments were possible in 7.5 M urea, behave in a similar manner to those shown in Figure 3. The ability to saturate the C_α chemical shifts in high denaturant is the principle evidence that an unfolding transition has occurred in the C-terminal half of FlgM. Conversely, for residues in the N-terminal half of FlgM, this is not the case. Several of these residues were assigned and show no titration behavior in the presence of 7.5 M urea. This is illustrated in Figure 2 by comparing the clear bars (no urea) with the black bars (7.5 M urea) for residues Q30−S38. Clearly, for these residues, the deviation in the C_α chemical shifts from no denaturant to high denaturant is insignificant.

When titrated with urea, the C_α chemical shifts, for most of the residues between M60−G73 and A83−A90, maintain a helical bias and never reach their random coil chemical shifts (Figure 5). In the absence of denaturant, the C_α chemical shifts for residues M60−G73 and A83−A90 are 50 ± 10% of the values expected for residues in a helical

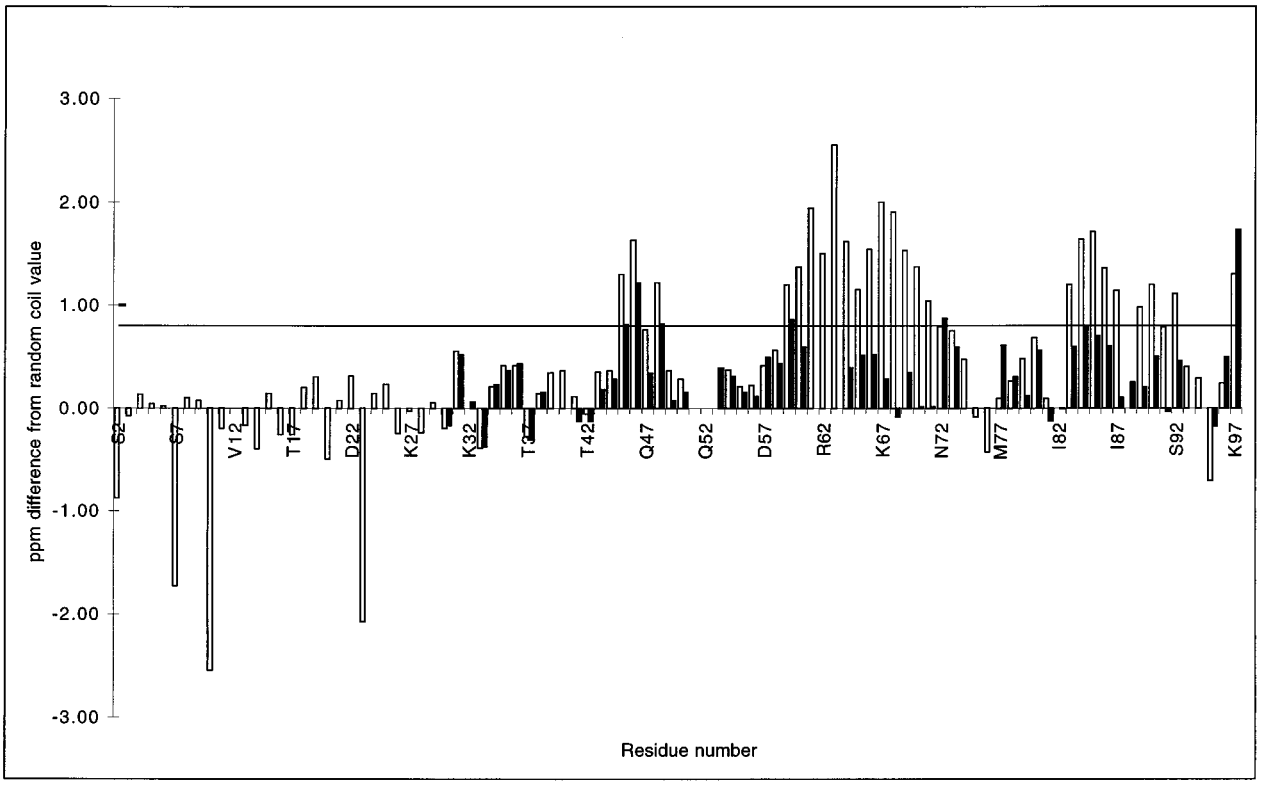

FIGURE 2: FlgM C_α chemical shift differences from random coil in no urea (clear bars) and 7.5 M urea (black bars). The dashed line is the cutoff for the helical CSI.

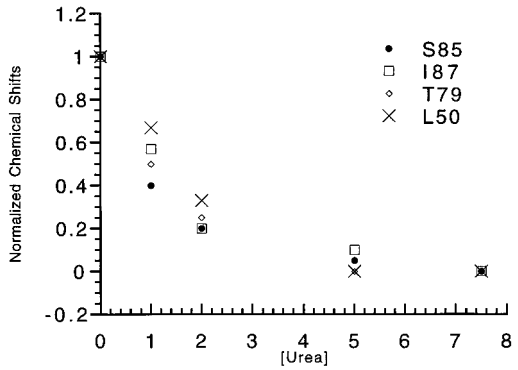

FIGURE 3: Plots of the normalized C_α chemical shifts versus the molar concentration of urea for residues S85, I87, T79, and L50. The C_α chemical shifts were normalized first by taking the difference between a residue's C_α chemical shifts at all urea concentrations and the C_α chemical shifts in 7.5 M urea. For each residue, this value was then divided by the difference in the C_α chemical shift at 0 and 7.5 M urea, producing a curve for all residues that begins at 1 and ends at 0.

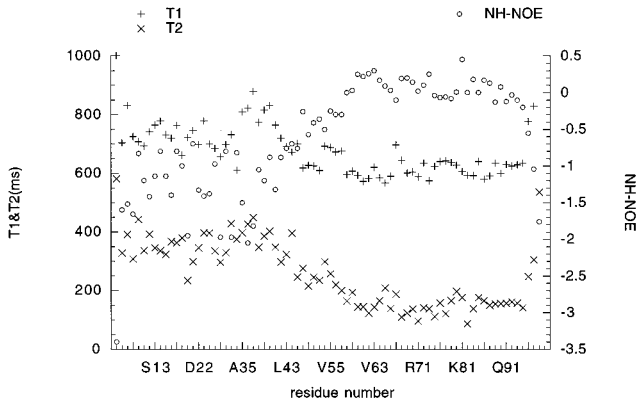

FIGURE 4: Plot of T_1, T_2, and the heteronuclear NOE values for FlgM.

conformation, which are between 3 and 4 Δppm. In the presence of high denaturant, the C_α chemical shifts for these same residues are 20 ± 10% of the value expected for residues in a helical conformation. This can be compared with C_α chemical shifts for most of the residues in the N-terminal half of FlgM, which, in the absence of denaturant, are within 0.5 ppm of the random coil value.

Relaxation Properties of FlgM. The relaxation parameters, T_1, T_2, and the heteronuclear NOE, were measured for all detectable backbone amide hydrogens in FlgM. Unambiguous intensity measurements were possible for resonances from 78 of the 93 non-proline residues. Figure 4 is a plot of T_1, T_2, and the heteronuclear NOE for these residues. These three parameters were extracted from the data as described under Materials and Methods. There are notable differences, between the N- and C-terminal halves of FlgM, for all three relaxation parameters, reflecting the structural and dynamic differences between the two halves of the molecule. The average T_2 for residues D4−S44 is 368 ± 60 ms and for residues S56−L94 is 153 ± 31 ms. The average T_1 for residues D4−S44 is 747 ± 72 ms and for residues S56−L94 is 613 ± 30 ms. All the heteronuclear NOE values for residues D4−S44 are large and negative, and many of the heteronuclear NOE values between S56 and L94 are small and positive.

Spectral Density Analysis of FlgM. The values of the reduced spectral density function for FlgM were calculated and are illustrated in Figure 5. According to the method of Farrow et al. (*13*), the contributions of the high-frequency terms to the relaxation rates have been collected under the single term $J(\omega_H)$. The flexibility along the protein backbone can be characterized simply by correlating the spectral

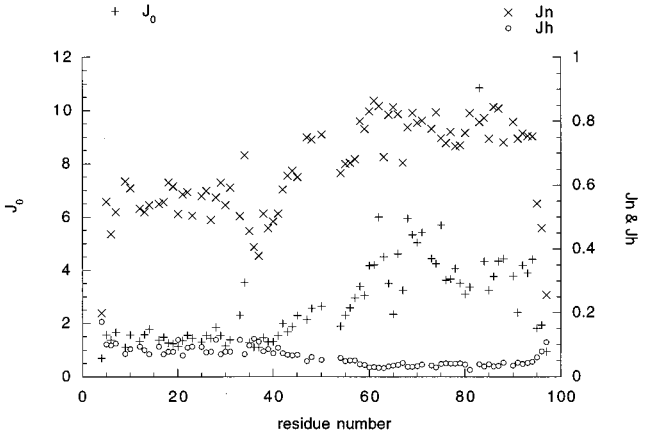

FIGURE 5: Plot of the spectral density values versus residue number for FlgM. J_0 refers to $J(0)$; Jn refers to $J(\omega_N)$; and Jh refers to $J(\omega_H)$.

density values with the protein sequence. The collective behavior for all the values of the three spectral density parameters indicates greater internal motion for the N-terminal half of FlgM as compared to the C-terminal half. The increase in $J(0)$ for the C-terminal half of FlgM can also be interpreted as an increase in molecular motions on the microsecond to millisecond time scale. This is consistent with a conformational transition between a helical structure and less ordered structures for M60−G73 and A83−A90. A close examination of $J(0)$ and $J(\omega_N)$ suggests two motional regions bracket the observed helical sections, and, over the entire sequence, there appear to be two other regions with distinct tumbling behavior. Residues D4−Q30 are certainly representative of an almost completely unfolded region of the protein, and the region between S40 and M60 shows a steady increase in the spectral density values. This steady increase reflects a progressive constraining of the NH bond vectors, until motions typical of the C-terminal domain are reached. The trend is paralleled in the relaxation rates and is not unlike what Zhou et al. (*26*) observed for the flexible linker, in the histidine autokinase CheA, which connects the phosphotransfer domain to the CheY binding domain. The principal difference here is that the flexible linker between the two functional domains of FlgM connects an almost completely unfolded N-terminal half to a partially folded C-terminal half.

Model-Free Analysis. The relaxation data were also analyzed using the model-free approach of Lipari and Szabo (*14*). It is important to emphasize the qualitative relevance of this approach for a mostly unfolded protein like FlgM. A global τ_m was never optimized, and instead this parameter is treated as an "effective local" correlation time for each residue. This is similar to the approach of Alexandrescu and Shortle (*12*), with the exception that in the current analysis the order parameter is not held at a fixed value. The calculated values of the correlation time for the overall motion, τ_m, and the order parameter, S^2, are shown in Figure 6a,b. The values of τ_m and S^2 were averaged between residues D4−S44 and S56−L94. These regions were selected because the standard deviations in τ_m and S^2 were minimized and because the regions constitute the two functional domains of FlgM. The average τ_m for residues D4−S44 is 3.61 ± 0.61 ns. This is significantly faster than the average τ_m for residues S56−L94 which is 6.29 ± 1.15 ns. The average S^2 for residues D4−S44 and S56−L94 is

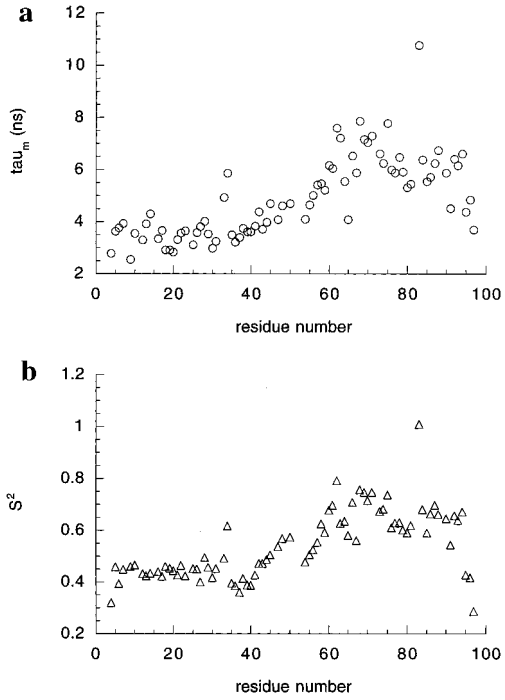

FIGURE 6: (a) Plot of the correlation time for overall motion, τ_m, for the residues in FlgM. (b) Plot of the order parameter, S^2, for the residues in FlgM.

0.44 ± 0.05 and 0.66 ± 0.08, respectively. For both halves of FlgM, the average values of S^2 and τ_m are larger than expected for 2 unfolded domains that are about 50 residues long and tumbling independently (*13*). This suggests that even though the tumbling behavior of the two halves of FlgM are distinct, they are not independent.

DISCUSSION AND CONCLUSIONS

This has been a report of the resonance assignments, dynamics, and average secondary structure of the anti-sigma factor FlgM. Using the C_α chemical shifts, two regions were identified between M60−G73 and A83−A90 that contained α-helical structure. These two regions also contained the majority of medium-range NOEs that were present in FlgM. Previous studies have shown M60−G73 and A83−A90 are essential for the anti-sigma factor activity of FlgM. Partial activity of a 24 amino acid fragment between E64−R88 and point mutants at positions L66, I82, and S85, that dramatically reduced the *in vivo* activity of FlgM, is evidence these regions are important for FlgM function (*5*, *27*). The C_α chemical shifts for the N-terminal half of FlgM closely resemble what is expected for a random coil. A few scattered residues have large chemical shifts, but the majority are within 0.5 ppm of the random coil value (Figure 2). The N-terminal half of FlgM is essential for flagella-specific export, and the lack of structure observed may be important for this function (*27*).

A comparison of the C_α chemical shifts for FlgM residues M60−G73 and A83−A90 with the helical C_α chemical shifts from Wishart and Sykes (*16*) suggests the helices in FlgM are not fully formed (data not shown). This hypothesis is confirmed by the relaxation experiments, which indicate the C-terminal half of FlgM is flexible. Because the $^{15}N-^{1}H$ correlation spectrum of FlgM shows a single resonance for each residue (Figure 1), the fluctuations between the various

conformations of FlgM are likely to occur faster than the millisecond time scale. This assumption does not address the possibility that a given conformation might give rise to a distinct chemical shift with an undetectable intensity. However, the S/N for all FlgM experiments was >200. Therefore, the C_α chemical shifts are an average from at least 99% of the conformations available to the protein.

Yang and Kay (*28*) have recently developed a method for predicting conformational entropy changes, between the folded and unfolded states of a protein, based on observed changes in S^2. This made it possible to further ascertain the role conformational entropy plays in determining the strength of the interaction between FlgM and σ^{28}. For all residue types, Yang and Kay (*28*) observed an average change in S^2, between the unfolded and the folded state, of 0.38 ± 0.17. From this value, they predict an average conformational entropy change of 2.87 cal (mol of residue)$^{-1}$ K^{-1}. This value is similar to what has been estimated for protein folding using a variety of techniques (*29*). The average S^2 for FlgM residues S56−L94 is 0.66 ± 0.08, and all of these residue are involved in binding to σ^{28} (*5*). Because of the size of the FlgM/σ^{28} complex (38 kDa), it was not possible to measure the relaxation parameters of bound FlgM. However, if a bound value for S^2 of 0.85 is assumed for residues S56−L94, the change in conformational entropy is 1.68 cal (mol of residue)$^{-1}$ K^{-1}. Therefore, the energy required, at 25 °C, to immobilize the 38 residues from S56−L94 is approximately 19 kcal/mol. This analysis considers each residue an independent contributor to the entropy change. This is most likely an oversimplification, but provides a useful qualitative picture of the entropic cost for FlgM residues being rigidly held by σ^{28}.

Based on the data presented in this paper, it appears that FlgM lacks the necessary stabilizing interactions to fold into a unique structure, and it has many of the features seen in folding intermediates of other proteins (*30*, *31*). That is, some reasonable percentage of secondary structure appears to exist in a partially collapsed state. However, it seems equally relevant to compare the results from the urea titration of the helical regions in the C-terminal half of FlgM with those for short α-helix-containing peptides. Scholtz et al. (*32*) measured urea unfolding for a homologous series of helical peptides with the repeating sequence Ala-Glu-Ala-Ala-Lys-Ala and chain lengths varying from 14 to 50 residues. They observed a change in the nature of the unfolding transition as they increased the chain length. Apparently, the cooperativity of the observed unfolding transitions was dependent on the length of the peptides. Peptides with 14 residues or less melted uncooperatively, with cooperative transitions occurring as the peptide length was increased past 20 residues. Both of the helical segments in FlgM melt uncooperatively and are less than 14 residues in length. This comparison suggests the unfolding of the helical segments in FlgM is largely governed by local interactions involving only a few residues.

The family progenitor of σ^{28}, σ^{70}, contains an autoinhibitory domain that performs a function similar to FlgM. This domain is contained within region 1.1 of σ^{70} and is thought to interact with its own DNA binding domain to inhibit specific binding activity. When region 1.1 is removed, σ^{70} can bind DNA in the absence of polymerase, an observation supporting this hypothesis (*33*). There is no apparent sequence homology between FlgM and region 1.1 of σ^{70}. However, in the recently solved crystal structure of a fragment of σ^{70}, region 1.1 was observed to be disordered (*34*). Given the structural and functional similarities between FlgM and region 1.1 of σ^{70}, it is not unreasonable to suggest that both FlgM and σ^{28} evolved from σ^{70}.

ACKNOWLEDGMENT

We gratefully acknowledge Hongjun Zhou for writing the FORTRAN programs used in the analysis of the relaxation data.

SUPPORTING INFORMATION AVAILABLE

The chemical shifts and dynamic parameters for FlgM are included in pages 1−9 of the supporting information for this article. Ordering information is given on any current masthead page.

REFERENCES

1. Gillen, K. L., and Hughes, K. T. (1991) *J. Bacteriol. 173*, 2301−2310.
2. Ohnishi, K., Kutsukake, K., Suzuki, H., and Iino, T. (1991) *Mol. Gen. Genet. 221*, 139−147.
3. Hughes, K. T., Gillen, K. L., Semon, M. J., and Karlinsey, J. E. (1993) *Science 262*, 1277−1280.
4. Kutsukake, K. (1994) *Mol. Gen. Genet. 243*, 605−612.
5. Daughdrill, G. W., Chadsey, M. S., Karlinsey, J. E., Hughes, K. T., and Dahlquist, F. W. (1997) *Nat. Struct. Biol. 4(4)*, 285−291.
6. Dreissen, A. J. M. (1994*) J. Membr. Biol. 142*, 145−159.
7. Cho, H. S., Liu, C. W., Damberger, F. F., Pelton, J. G., Nelson, H. C. M., and Wemmer, D. E. (1996) *Protein Sci. 5*, 262−269.
8. Habazett, J., Myers, L. C., Yuan, F., Verdine, G. L., and Wagner, G. (1996) *Biochemistry 35*, 9335−9348.
9. Sem, D. S., Casimiro, D. R., Kliewer, S. A., Provencal, J., Evans, R. E., and Wright, P. E. (1997) *J. Biol. Chem. 272-(29)*, 18038−18043.
10. R. S., Spolar, and Record, M. T., Jr. (1994) *Science 263*, 777−784.
11. Schulz, G. E. (1979) *Molecular Mechanisms of Biological Recognition*, pp 79−94 Elsevier/North-Holland Biomedical Press, Amsterdam, The Netherlands.
12. Alexandrescu, A. T., and Shortle, D. (1994) *J. Mol. Biol. 242*, 527−546.
13. Farrow, N. A., Zhang, O., Forman-Kay, J. D., and Kay, L. E. (1997) *Biochemistry 36*, 2390−2402.
14. Lipari, G., and Szabo, A. (1982) *J. Am. Chem. Soc. 104*, 4546−4559.
15. Kay, L. E., Torchia, D. A., and Bax, A. (1989) *Biochemistry 28(23)*, 8972−8979.
16. Wishart, D. S., and Sykes, B. D. (1994) *Methods Enzymol. 239*, 363−392.
17. Marion, D., Kay, L. E., Sparks, S. W., Torchia, D. A., and Bax, A. (1989a) *J. Am. Chem. Soc. 111*, 1515−1517.
18. Zuiderweg, E. R. P., and Fesik, S. W. (1989) *Biochemistry 28*, 2387−2391.
19. Cavanagh, J., Chazin, W. J., and Rance, M. (1989) *J. Magn. Reson. 87*, 110−131.
20. Marion, D., Driscoll, P. C., Kay, L. E., Wingfield, P. T., Bax, A., Gronenborn, A. M., and Clore, G. M. (1989b) *Biochemistry 28*, 6150−6156.
21. Muhandiram, D. R., and Kay, L. E. (1994) *J. Magn. Res., Ser. B 103*, 203−216.

22. Kay, L. E., Xu, G. Y., and Yamazaki, T. (1994) *J. Magn. Res., Ser. A 109*, 129−133.
23. Bodenhausen, G., and Ruben, D. J. (1980) *Chem. Phys. Lett. 69*, 185−199.
24. Kay, L. E., Keifer, P., and Sarinen, T. (1992) *J. Am. Chem. Soc. 114*, 10663−10665.
25. Wüthrich, K. (1986) *NMR of Proteins and Nucleic Acids*, Wiley, New York.
26. Zhou, H., McEvoy, M. M., Lowry, D. L., Swanson, R. V., Simon, M. I., and Dahlquist, F. W. (1996) *Biochemistry 35*, 433−443.
27. Iyoda, S., and Kutsukake, K. (1995) *Mol. Gen. Genet. 249*, 417−424.
28. Yang, D., and Kay, L. E. (1996) *J. Mol. Biol. 263*, 369−382.
29. Doog, A. J., and Sternberg, M. J. E. (1995) *Protein Sci. 4*, 2247−2251.
30. Baldwin, R. L. (1996) *Fold. Des. 1(1)*, R1−8.
31. Kuwajima, K. (1996) *FASEB J. 10(1)*, 162−169.
32. Scholtz, J. M., Barrick, D., York, E. J., Stewart, J. M., and Baldwin, R. L. (1995) *Proc. Natl. Acad. Sci. U.S.A. 92*, 185−189.
33. Dombroski, A. J., Walter, W. A., and Gross, C. A. (1993) *Genes Dev. 7*, 2446−2455.
34. Malhotra, A., Severinova, E., and Darst, S. A. (1996) *Cell 87*, 127−136.

BI971952T